

## Spectroscopy of $^{26}\text{F}$ to Probe Proton-Neutron Forces Close to the Drip Line

A. Lepailleur,<sup>1</sup> O. Sorlin,<sup>1</sup> L. Caceres,<sup>1</sup> B. Bastin,<sup>1</sup> C. Borcea,<sup>2</sup> R. Borcea,<sup>2</sup> B. A. Brown,<sup>3</sup> L. Gaudefroy,<sup>4</sup> S. Grévy,<sup>5</sup>  
G. F. Grinyer,<sup>1</sup> G. Hagen,<sup>6,7</sup> M. Hjorth-Jensen,<sup>3,8</sup> G. R. Jansen,<sup>6,7</sup> O. Llidoo,<sup>1</sup> F. Negoita,<sup>2</sup> F. de Oliveira,<sup>1</sup>  
M.-G. Porquet,<sup>9</sup> F. Rotaru,<sup>2</sup> M.-G. Saint-Laurent,<sup>1</sup> D. Sohler,<sup>10</sup> M. Stanoiu,<sup>2</sup> and J. C. Thomas<sup>1</sup>

<sup>1</sup>Grand Accélérateur National d'Ions Lourds (GANIL), CEA/DSM—CNRS/IN2P3, BP 55027, F-14076 Caen Cedex 5, France

<sup>2</sup>IFIN-HH, P.O. Box MG-6, 76900 Bucharest-Magurele, Romania

<sup>3</sup>National Superconducting Cyclotron Laboratory and Department of Physics and Astronomy, Michigan State University, East Lansing, Michigan 48824, USA

<sup>4</sup>CEA, DAM, DIF, F-91297 Arpajon, France

<sup>5</sup>Centre d'Études Nucléaires de Bordeaux Gradignan-UMR 5797, CNRS/IN2P3, Université de Bordeaux 1, Chemin du Solarium, BP 120, 33175 Gradignan, France

<sup>6</sup>Physics Division, Oak Ridge National Laboratory, Oak Ridge, Tennessee 37831, USA

<sup>7</sup>Department of Physics and Astronomy, University of Tennessee, Knoxville, Tennessee 37996, USA

<sup>8</sup>Department of Physics and Center of Mathematics for Applications, University of Oslo, N-0316 Oslo, Norway

<sup>9</sup>CSNSM, CNRS/IN2P3, Université Paris-Sud, F-91405 Orsay, France

<sup>10</sup>Institute of Nuclear Research of the Hungarian Academy of Sciences, P.O. Box 51, Debrecen, H-4001, Hungary

(Received 29 November 2012; published 19 February 2013)

A long-lived  $J^\pi = 4_1^+$  isomer,  $T_{1/2} = 2.2(1)$  ms, has been discovered at 643.4(1) keV in the weakly bound  $^{26}\text{F}$  nucleus. It was populated at Grand Accélérateur National d'Ions Lourds in the fragmentation of a  $^{36}\text{S}$  beam. It decays by an internal transition to the  $J^\pi = 1_1^+$  ground state [82(14)%], by  $\beta$  decay to  $^{26}\text{Ne}$ , or  $\beta$ -delayed neutron emission to  $^{25}\text{Ne}$ . From the  $\beta$ -decay studies of the  $J^\pi = 1_1^+$  and  $J^\pi = 4_1^+$  states, new excited states have been discovered in  $^{25,26}\text{Ne}$ . Gathering the measured binding energies of the  $J^\pi = 1_1^+ - 4_1^+$  multiplet in  $^{26}\text{F}$ , we find that the proton-neutron  $\pi 0d_{5/2} \nu 0d_{3/2}$  effective force used in shell-model calculations should be reduced to properly account for the weak binding of  $^{26}\text{F}$ . Microscopic coupled cluster theory calculations using interactions derived from chiral effective field theory are in very good agreement with the energy of the low-lying  $1_1^+$ ,  $2_1^+$ ,  $4_1^+$  states in  $^{26}\text{F}$ . Including three-body forces and coupling to the continuum effects improve the agreement between experiment and theory as compared to the use of two-body forces only.

DOI: [10.1103/PhysRevLett.110.082502](https://doi.org/10.1103/PhysRevLett.110.082502)

PACS numbers: 21.60.Cs, 23.35.+g, 21.60.De, 23.20.Lv

**Introduction.**—Understanding the boundaries of the nuclear landscape and the origin of magic nuclei throughout the chart of nuclides are overarching aims and intellectual challenges in nuclear physics research [1]. These are major motivations that drive the developments of present and planned rare-isotope facilities. Studying the evolution of binding energies for the ground and first few excited states in atomic nuclei from the valley of stability to the drip line (where the next isotope is unbound with respect to the previous one) is essential to achieve these endeavors. Understanding these trends and providing reliable predictions for nuclei that cannot be accessed experimentally require a detailed understanding of the properties of the nuclear force [2,3].

In the oxygen isotopes, recent experiments have shown that the drip line occurs at the doubly magic  $^{24}\text{O}_{16}$  [4–6], as  $^{25,26}\text{O}$  are unbound [7–9]. The role of tensor and three-body forces was emphasized in Refs. [10,11] to account for the emergence of the  $N = 16$  gap at  $^{24}\text{O}_{16}$  and the “early” appearance of the drip line in the O isotopic chain, respectively. On the other hand, with the exception of  $^{28}\text{F}$  [12] and  $^{30}\text{F}$ , which are unbound, six more neutrons can be added in the F isotopic chain before reaching the drip line at  $^{31}\text{F}_{22}$

[13]. One can therefore speculate that the extension of the drip line between the oxygen and fluorine, as well as the odd-even binding of the fluorine isotopes, arise from a delicate balance between the two-body proton-neutron and neutron-neutron interactions, the coupling to the continuum [14] effects, and the three-body forces [15–19].

The study of  $^{26}\text{F}$ , which is bound by only 0.80(12) MeV [20], offers a unique opportunity to investigate several aspects of the nuclear force. The  $^{26}\text{F}$  nucleus can be modeled using a simplified single-particle (SP) description as a closed  $^{24}\text{O}$  core plus a *deeply bound* proton in the  $\pi 0d_{5/2}$  orbital [ $S_\pi(^{25}\text{F}) \simeq -15.1(3)$  MeV [21]] plus an *unbound* neutron [ $S_\nu(^{25}\text{O}) \simeq 770_{-10}^{+20}$  keV [7]] in the  $\nu 0d_{3/2}$  orbital. This simplified picture arises from the fact that the first excited state in  $^{24}\text{O}$  lies at 4.47 MeV [4,6] and the  $\pi 0d_{5/2}$  and  $\nu 0d_{3/2}$  single-particle energies are well separated from the other orbitals. The low-lying  $J^\pi = 1_1^+$ ,  $2_1^+$ ,  $3_1^+$ ,  $4_1^+$  states in  $^{26}\text{F}$  thus arise, to a first approximation, from the interactions of nucleons in the  $\pi 0d_{5/2}$  and  $\nu 0d_{3/2}$  orbits.

Present experimental knowledge concerning the members of the  $J^\pi = 1_1^+$ ,  $2_1^+$ ,  $3_1^+$ ,  $4_1^+$  multiplet in  $^{26}\text{F}$  is as follows. A  $J^\pi = 1_1^+$  assignment has been proposed in

Ref. [22] for the ground state of  $^{26}\text{F}$  from the observation that its  $\beta$  decay proceeds to the  $J^\pi = 0_1^+$ ,  $J^\pi = 2_1^+$  states and a tentative  $J^\pi = 0_2^+$  state in  $^{26}\text{Ne}$ . The half-life of  $^{26}\text{F}$  was found to be  $10.2 \pm 1.4$  ms with a  $P_n$  value of  $11 \pm 4\%$  [22]. A mass excess  $\Delta M$  of 18.680(80) MeV was determined for  $^{26}\text{F}$  in Ref. [20] using the time-of-flight technique. The  $J^\pi = 2_1^+$  state was discovered at 657(7) keV [23] from the fragmentation of  $^{27,28}\text{Na}$  nuclei. In addition a charge-exchange reaction with a  $^{26}\text{Ne}$  beam was used in Ref. [24] to study unbound states in  $^{26}\text{F}$ . In this reaction, a neutron capture to the  $\nu d_{3/2}$  orbital and a proton removal from the  $\pi d_{5/2}$  (which are both valence orbitals) are likely to occur leading to the  $J^\pi = 1_1^+ - 4_1^+$  states. The resonance observed at 271(37) keV above the neutron emission threshold [24] could tentatively be attributed to the  $J^\pi = 3_1^+$  in  $^{26}\text{F}$ , as it was the only state of the  $J^\pi = 1_1^+ - 4_1^+$  that was predicted to be unbound. With the determination of the binding energies of the  $J^\pi = 1_1^+ - 3_1^+$  states, the only missing information is the energy of the  $J^\pi = 4_1^+$  state. In this Letter, we demonstrate that the  $4_1^+$  state is isomeric and decays by competing internal transition and  $\beta$  decay. Its binding energy is determined and those of the  $1_1^+ - 2_1^+$  states are reevaluated. The comparison of the measured binding energies of the  $J^\pi = 1_1^+ - 4_1^+$  states with two theoretical approaches, the nuclear shell model and the coupled cluster (CC) theory, provides a stringent test of the nuclear forces, where a large proton-to-neutron binding energy asymmetry is present.

**Experiment.**—The  $^{26}\text{F}$  nuclei were produced through the fragmentation of a 77.6 MeV/A  $^{36}\text{S}^{16+}$  primary beam with a mean intensity of  $2 \mu\text{Ae}$  in a  $237 \text{ mg/cm}^2$  Be target. They were selected by the LISE [25] spectrometer at GANIL, in which a wedge-shaped degrader of  $1066 \mu\text{m}$  was inserted at the intermediate focal plane. The produced nuclei were identified from their energy loss in a stack of Si detectors and by their time of flight with respect to the GANIL cyclotron radio frequency. The production rate of  $^{26}\text{F}$  was 6 pps with a purity of 22% and a momentum acceptance of 2%. Other transmitted nuclei, ranked by decreasing order of production, were  $^{28}\text{Ne}$ ,  $^{29}\text{Na}$ ,  $^{27}\text{Ne}$ ,  $^{24}\text{O}$ ,  $^{22}\text{N}$ , and  $^{30}\text{Na}$ . They were implanted in a 1 mm-thick double-sided Si stripped detector (DSSSD) composed of 256 pixels (16 strips in the  $X$  and  $Y$  directions) of  $3 \times 3 \text{ mm}^2$ —each located at the final focal point of LISE. This detector was used to detect the  $\beta$  particles in strips  $i$ ,  $i \pm 1$  following the implantation of a radioactive nucleus in a given pixel  $i$ . With an energy threshold of  $\sim 80$  keV in the individual strips, a  $\beta$  efficiency of 64(2)% was achieved for  $^{26}\text{F}$ , which was implanted at the central depth of the DSSSD. The  $\beta$  efficiency has been determined from the comparison of the intensity of a given  $\gamma$  ray belonging to the decay of  $^{26}\text{F}$  gated or not on a  $\beta$  ray. Four clover Ge detectors of the EXOGAM array [26] surrounded the DSSSD to detect the  $\gamma$  rays, leading to a  $\gamma$ -ray efficiency of 6.5% at 1 MeV.

The  $\gamma$ -ray spectra obtained up to 2 ms after the implantation of a radioactive nucleus are shown in Fig. 1(a). In this frame the upper (middle) spectrum is obtained by requiring that  $^{26}\text{F}$  (all except  $^{26}\text{F}$ ) precedes the detection of a  $\gamma$  ray. A delayed  $\gamma$ -ray transition at 643.4(1) keV is clearly observed after the implantation of  $^{26}\text{F}$ . The bottom spectrum of Fig. 1(a) is operated in a similar condition as the top one, with the additional requirement that  $\gamma$  rays are detected in coincidence with a  $\beta$  transition. As the 643.4(1) keV is not in coincidence with  $\beta$  particles it must correspond to an internal transition (IT) deexciting an isomeric state in  $^{26}\text{F}$ , which has a half-life of 2.2(1) ms [see Fig. 1(b)]. This isomer is likely the  $4^+$  state we are searching for. It either decays directly to the  $1^+$  ground state, hereby establishing the  $4^+$  state at 643.4(1) keV, or, alternatively, the 643.4(1) keV energy may correspond, but with a weak level of confidence, to the 657(7) keV state observed in Ref. [23]. In this hypothesis, the isomerism of the  $4^+$  state would be due to the emission of a very low energy  $4^+ \rightarrow 2^+$  transition (up to 10 keV to ensure having a long-lived isomer), then followed by the  $2^+ \rightarrow 1^+$  transition. In either case, the excitation energy of the  $4^+$  state lies at approximately 650(10) keV.

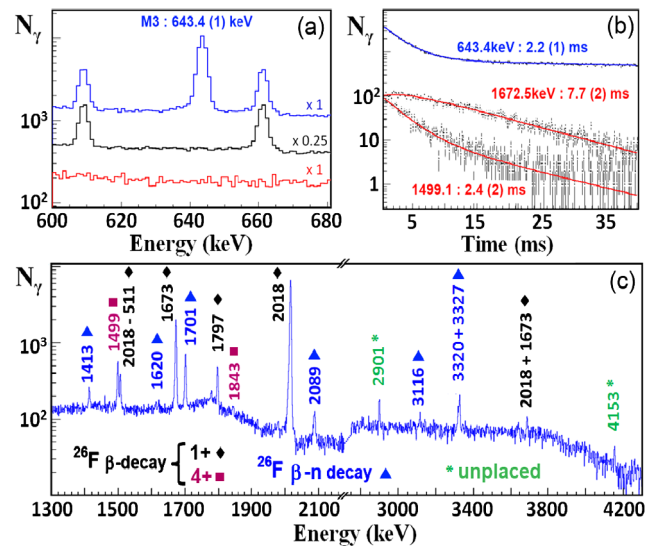


FIG. 1 (color online). (a)  $\gamma$ -ray spectra obtained up to 2 ms after the implantation of  $^{26}\text{F}$  (upper spectrum), or after the implantation of any nucleus except  $^{26}\text{F}$  (middle spectrum). The bottom spectrum shows the  $\beta$ -gated  $\gamma$  rays following the implantation of  $^{26}\text{F}$ . (b) Time spectra between implanted  $^{26}\text{F}$  and  $\gamma$  rays, from which half-lives can be deduced. The  $4^+ \rightarrow 1^+$  transition in  $^{26}\text{F}$  [643.4(1) keV] and the  $4^+ \rightarrow 2_1^+$  transition in  $^{26}\text{Ne}$  [1499.1(4) keV] have the same half-life, while the  $2_2^+ \rightarrow 2_1^+$  transition in  $^{26}\text{Ne}$  [1672.5(3) keV] has a larger half-life. (c)  $\beta$ -gated  $\gamma$ -ray spectrum following the implantation of  $^{26}\text{F}$  up to 30 ms. Symbols (colors) indicate which lines correspond to the  $\beta$  decay of the  $1^+$  (black diamonds) and  $4^+$  (red squares) or to the  $\beta$  delayed-neutron branch (blue triangles). The same color codes are used in the decay scheme of Fig. 2. Two lines (green stars) could not be placed in the decay scheme of  $^{26}\text{F}$ .

The decay of this  $4^+$  state occurs through a competition between an IT and  $\beta$  decay to two states in  $^{26}\text{Ne}$ . The half-lives corresponding to the IT [2.2(1) ms] as well as to the 1499.1(4) keV [2.4(2) ms] and 1843.4(8) keV [2(1) ms] peaks of Fig. 1(c) are the same. These two transitions are seen in mutual coincidences, as well as with the 2017.6(3) keV  $\gamma$  ray, previously assigned to the  $2_1^+ \rightarrow 0_1^+$  transition in  $^{26}\text{Ne}$  in Ref. [22]. This establishes two levels at 3516.7(4) keV and 5360.1(9) keV in  $^{26}\text{Ne}$  as shown in Fig. 2 (see the Supplemental Material [27]). Following the Gamow-Teller  $\beta$ -decay selection rules the  $4^+$  isomer should mainly proceed to the  $J^\pi = 4_1^+$  state in the vibrator  $^{26}\text{Ne}$  nucleus, which we attribute to the 3516.7(4) keV state.

All other observed transitions in Fig. 1(c) from  $^{26}\text{F}$  belong to the decay of the  $1^+$  ground state, as their half-lives differ significantly from that of the  $4^+$  isomeric state. The two  $\gamma$ -ray transitions at 1672.5(3) keV and 1797.1(4) keV were found to be in coincidence with the 2017.6(3) keV transition, but not in mutual coincidence. This establishes two levels at 3690.1(4) keV and 3814.7(5) keV that have compatible half-lives of 7.7(2) ms and 7.8(5) ms, respectively. These states presumably belong to the two-phonon multiplet of states  $J^\pi = 0_2^+, 2_2^+, 4_1^+$ , among which the 3516.7(4) keV one was assigned to  $J^\pi = 4_1^+$  (see above). Using in-beam  $\gamma$ -ray spectroscopy from the fragmentation of a  $^{36}\text{S}$  beam [28], the feeding of the 3516.7(4) keV level was the largest, that of the 3689.8(4) keV state was weaker, while the state at

3814.7(5) keV was not fed. As this method mainly produces yrast states, i.e., states having the highest spin value in a given excitation energy range, we ascribe  $J^\pi = 2_2^+$  to the state at 3690.1(4) keV, in accordance with Ref. [29], and  $J^\pi = 0_2^+$  to the state at 3814.7(5) keV. The fitting of the decay half-lives must include the direct  $1_1^+$  decay of  $^{26}\text{F}$  as well as the partial feeding from the  $4_1^+ \rightarrow 1_1^+$  transitions. This leads to a growth at the beginning of the time spectrum [Fig. 1(b) for the 1673 keV  $\gamma$  ray], which depends on the isomeric ratio  $R$  and on the internal transition coefficient IT. These parameters are furthermore constrained by the amount of the 643.4(1) keV  $\gamma$  rays observed per implanted  $^{26}\text{F}$  nucleus, leading to  $R = 42(8)\%$  and  $\text{IT} = 82(11)\%$ .

The  $\beta$  feedings derived from the observed  $\gamma$ -ray intensities are given in Fig. 2. In the  $\beta$ -delayed neutron branch of  $^{26}\text{F}$  to  $^{25}\text{Ne}$ , some levels observed in Refs. [22,30,31] are confirmed, while a new state is proposed at 3114.1(8) keV as the 1413.2(7) keV and 1700.9(4) keV  $\gamma$  rays are in coincidence and the summed  $\gamma$ -ray energy is observed at 3116(2) keV. A  $P_n$  value of 16(4)% [consistent with  $P_n = 11(4)\%$  [22]] is extracted for  $^{26}\text{F}$  from the observation of the 979.7 keV  $\gamma$  ray in the granddaughter nucleus  $^{25}\text{Na}$  whose branching ratio of 18.1(19)% was determined in Ref. [32]. We therefore adopt a mean value of  $P_n = 13.50(40)\%$  for  $^{26}\text{F}$ . The proposed level scheme and branching ratios agree relatively well with the shell-model calculation shown on the right side of Fig. 2.

The discovery of this new isomer has an important consequence on the determination of the atomic mass of the  $^{26}\text{F}$  ground state as well as on the interpretation of the one-neutron knockout cross sections from  $^{26}\text{F}$  of Ref. [33]. It is very likely that the measured atomic mass of Ref. [20] corresponds to a mixture of the ground and the isomeric states (unknown at that time). As the  $^{26}\text{F}$  nuclei were produced in the present work and that of Ref. [20] in similar fragmentation reactions involving a large number of removed nucleons, we can reasonably assume that the  $^{26}\text{F}$  isomeric ratio is the same in the two experiments. The shift in the  $^{26}\text{F}$  atomic mass as a function of the isomeric ratio  $R$  amounts to  $-6.43$  keV/%, which for  $R = 42(8)\%$  yields  $-270(50)$  keV.

*Discussion.*—The comparison between the experimental binding energies of these states can now be made with two theoretical approaches, the nuclear shell model and CC theory. The experimental (calculated) interactions elements arising from the coupling between a  $d_{5/2}$  proton and a  $d_{3/2}$  neutron, labeled  $\text{Int}(J)$ , are extracted from the experimental (calculated) binding energies (BE) as

$$\text{Int}(J) = \text{BE}(^{26}\text{F})_J - \text{BE}(^{26}\text{F}_{\text{free}}).$$

In this expression  $\text{BE}(^{26}\text{F}_{\text{free}})$  corresponds to the binding energy of the  $^{24}\text{O} + 1p + 1n$  system, in which the valence proton in the  $d_{5/2}$  orbit and the neutron in the  $d_{3/2}$  orbit do not interact. It can be written as

$$\text{BE}(^{26}\text{F}_{\text{free}}) = \text{BE}(^{25}\text{F})_{5/2^+} + \text{BE}(^{25}\text{O})_{3/2^+} - \text{BE}(^{24}\text{O})_{0^+}.$$

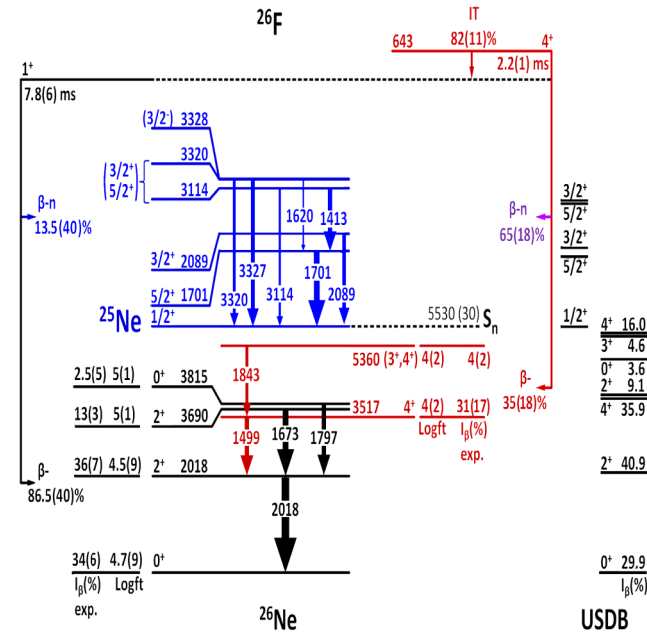


FIG. 2 (color online). Decay scheme obtained from the decays of the  $4^+$  (red) and  $1^+$  states (black) in  $^{26}\text{F}$  to  $^{26}\text{Ne}$  and  $^{25}\text{Ne}$  (blue). Shell-model predictions obtained with the USDB interaction are shown on the right-hand side. An expanded version of this figure, in which the decay schemes of the  $1^+$  and  $4^+$  states are split into two parts, can be seen in the Supplemental Material [27].

Using the relative binding energy of  $+0.77_{-10}^{+20}$  MeV [7] between  $^{24}\text{O}$  and  $^{25}\text{O}$ , the measured atomic masses in  $^{25}\text{F}$  and  $^{26}\text{F}$  [20], and the shift in energy due to the isomeric content (see above) it is found that the experimental value of  $\text{Int}(1)$  is  $-1.85(13)$  MeV. The values of  $\text{Int}(2) = -1.19(14)$  MeV and  $\text{Int}(4) = -1.21(13)$  MeV are obtained using the  $J^\pi = 2_1^+$  and  $J^\pi = 4_1^+$  energies of 657(7) keV and 643.4(1) keV, respectively. A value of  $\text{Int}(3) = -0.49(4)$  MeV is derived from the energy of the  $J^\pi = 3_1^+$  resonance with respect to the  $^{25}\text{F}$  ground state.

In the shell-model calculations of Refs. [34,35], the two-body matrix elements corresponding to interactions in the  $sd$  valence space are fitted to reproduce properties of known nuclei. Applying these interactions to nuclei not included in the global fits (such as bound and unbound states in  $^{26}\text{F}$ ) implies that shell-model calculations toward the drip lines can be viewed as predictions. Because of the strong coupling to the continuum and a likely absence of many-body correlations not included in the fits, these interactions may fail in reproducing properties of nuclei like  $^{26}\text{F}$ . Owing to its simple structure,  $^{26}\text{F}$  provides a unique possibility to probe the strength of the proton-neutron interaction close to the drip line. The wave functions of the  $J^\pi = 1_1^+ - 4_1^+$  states are composed of mainly (80%–90%) pure  $\pi 0d_{5/2} \otimes \nu 0d_{3/2}$  component. By calculating all states in the  $J^\pi = 1_1^+ - 4_1^+$  multiplet, it can be seen in Fig. 3 that the  $J^\pi = 1_1^+$  state is less bound than calculated by about 17% (8%) and that the multiplet of experimental states is compressed by about 25% (15%) compared with the USDA (USDB) calculations. This points to a weakening of the residual interactions, which caused the energy splitting between the members of the multiplet.

We have also performed microscopic CC [36,37] calculations for  $^{26}\text{F}$ . This method is particularly suited for nuclei with closed (sub)shells, and their nearest neighbors. Moreover, CC theory can easily handle nuclei in which

protons and neutrons have significantly different binding energies. To estimate the  $\pi 0d_{5/2} - \nu 0d_{3/2}$  interaction energy  $[\text{Int}(J)]$ , we use CC theory with singles and doubles excitations with perturbative triples corrections [38,39] for the closed-shell nucleus  $^{24}\text{O}$ , the particle-attached CC method for  $^{25}\text{O}$  and  $^{25}\text{F}$  [40] and the two-particle attached formalism for  $^{26}\text{F}$  [41]. We employ interactions from chiral effective field theory [42]. The effects of three-nucleon forces are included as corrections to the nucleon-nucleon interaction by integrating one nucleon in the leading-order chiral three-nucleon force over the Fermi sphere with a Fermi momentum  $k_F$  in symmetric nuclear matter [43]. The parameters recently established in the oxygen chain [16] are adopted in the present work. We use a Hartree-Fock basis built from  $N_{\text{max}} = 17$  major spherical oscillator shells with the oscillator frequency  $\hbar\omega = 24$  MeV. This is sufficiently large to achieve convergence of the calculations for all isotopes considered. Using two-body nucleon-nucleon forces we get the ground-state energy of  $^{26}\text{F}$  at  $-173.2$  MeV, which is underbound by  $\sim 11$  MeV compared to experiment. However, the relative spectra for the excited states are in fair agreement with experiment (see Fig. 3). In order to account for the coupling to the continuum in  $^{26}\text{F}$ , we use a real Woods-Saxon basis for the  $\nu 1s_{1/2}$  and  $\nu 0d_{3/2}$  partial waves [44]. The inclusion of continuum effects and three-nucleon forces improve the situation: the ground-state energy is at  $-177.07$  MeV, and the low-lying spectra are in very good agreement with experiment. The  $J^\pi = 3^+$  state in  $^{26}\text{F}$  is a resonance and to compute this state we need a Gamow-Hartree-Fock basis [45]. We are currently working on generalizing the two-particle attached CC implementation to a complex basis. Therefore, the interaction energy of the  $J = 3$  state is not shown in Fig. 3. Consistently with the shell-model calculations described above, a simple picture emerges from the microscopic CC calculations: about 85% of the  $1^+ - 4^+$  wave functions are composed of  $1s0d$ -shell components, in which configurations consisting of the  $\pi 0d_{5/2}$  and  $\nu 0d_{3/2}$  SP states play a major role.

*Conclusions.*—To summarize, a new  $J^\pi = 4_1^+$  isomer with a 2.2(1) ms half-life has been discovered at 643.4(1) keV. Its isomeric decay to the  $J^\pi = 1_1^+$  ground state and  $\beta$  decay to the  $J^\pi = 4_1^+$  state in  $^{26}\text{Ne}$  were observed. Gathering the  $\beta$ -decay branches observed from the  $J^\pi = 1_1^+$  and  $J^\pi = 4_1^+$  states, partial level schemes of  $^{26}\text{Ne}$  and  $^{25}\text{Ne}$  were obtained. In addition, the  $^{26}\text{F}$  nucleus is a benchmark case for studying proton-neutron interactions far from stability. The experimental states  $J = 1^+ - 4^+$  arising from the  $\pi d_{5/2} \otimes \nu d_{3/2}$  coupling in  $^{26}\text{F}$  are more compressed than the USDA and USDB shell-model results. The experimental  $J^\pi = 1_1^+, 2_1^+, 4_1^+$  states are less bound as well. These two effects point to a dependence of the effective two-body interaction used in the shell model as a function of the proton-to-neutron binding energy asymmetry. Coupled-cluster calculations including three-body

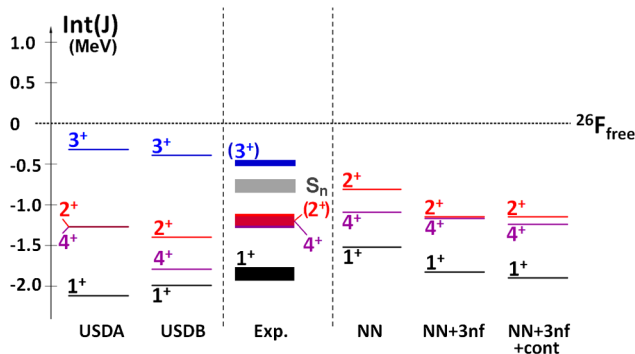


FIG. 3 (color online). Calculated and experimental interaction energies  $\text{Int}(1 - 4)$  in MeV in  $^{26}\text{F}$ . Shell-model calculations are shown in the first column using the USDA or USDB interactions, while the third column shows results obtained with CC calculations. Experimental results are in the center. The thickness of the lines corresponds to  $\pm 1\sigma$  error bar.

forces and coupling to the particle continuum are in excellent agreement with experiment for the bound low-lying states in  $^{26}\text{F}$ .

This work was partly supported by the Office of Nuclear Physics, U.S. Department of Energy (Oak Ridge National Laboratory), under Contracts No. DE-FG02-96ER40963 (University of Tennessee) and No. DE-SC0008499 (NUCLEI SciDAC-3 Collaboration), NSF Grant No. PHY-1068217, OTKA Contract No. K100835, a grant of the Romanian National Authority for Scientific Research, CNCS UEFISCDI, PN-II-RU-TE-2011-3-0051, as well as by FUSTIPEN (French-U.S. Theory Institute for Physics with Exotic Nuclei) under DOE Grant No. DE-FG02-10ER41700. Computer time was provided by the Innovative and Novel Computational Impact on Theory and Experiment (INCITE) program. This research used resources of the Oak Ridge Leadership Computing Facility located in the Oak Ridge National Laboratory, which is supported by the Office of Science of the Department of Energy under Contract No. DE-AC05-00OR22725 and used computational resources of the National Center for Computational Sciences, the National Institute for Computational Sciences, and the Notur project in Norway. The CENBG is gratefully acknowledged for the loan of the DSSSD detector. A.L. thanks V. Tripathi for communicating information which we used for calibration purposes.

- 
- [1] J. Erler, N. Birge, M. Kortelainen, W. Nazarewicz, E. Olsen, A.M. Perhac, and M. Stoitsov, *Nature (London)* **486**, 509 (2012).
- [2] O. Sorlin and M.-G. Porquet, *Prog. Part. Nucl. Phys.* **61**, 602 (2008); *Phys. Scr.* **T152**, 014003 (2013).
- [3] T. Baumann, A. Spyrou, and M. Thoennessen, *Rep. Prog. Phys.* **75**, 036301 (2012).
- [4] C.R. Hoffmann *et al.*, *Phys. Lett. B* **672**, 17 (2009).
- [5] R. Kanungo *et al.*, *Phys. Rev. Lett.* **102**, 152501 (2009).
- [6] K. Tshoo *et al.*, *Phys. Rev. Lett.* **109**, 022501 (2012).
- [7] C.R. Hoffman *et al.*, *Phys. Rev. Lett.* **100**, 152502 (2008).
- [8] E. Lunderberg *et al.*, *Phys. Rev. Lett.* **108**, 142503 (2012).
- [9] C. Caesar *et al.*, [arXiv:1209.0156](https://arxiv.org/abs/1209.0156).
- [10] T. Otsuka, T. Suzuki, J.D. Holt, A. Schwenk, and Y. Akaishi, *Phys. Rev. Lett.* **105**, 032501 (2010).
- [11] T. Otsuka, T. Suzuki, R. Fujimoto, H. Grawe, and Y. Akaishi, *Phys. Rev. Lett.* **95**, 232502 (2005).
- [12] G. Christian *et al.*, *Phys. Rev. Lett.* **108**, 032501 (2012).
- [13] S.M. Lukyanov and Yu.E. Penionzhkevich, *Phys. At. Nucl.* **67**, 1627 (2004) and references therein.
- [14] J. Dobaczewski, N. Michel, W. Nazarewicz, M. Płoszajczak, and J. Rotureau, *Prog. Part. Nucl. Phys.* **59**, 432 (2007).
- [15] G. Hagen, M. Hjorth-Jensen, G.R. Jansen, R. Machleidt, and T. Papenbrock, *Phys. Rev. Lett.* **109**, 032502 (2012).
- [16] G. Hagen, M. Hjorth-Jensen, G.R. Jansen, R. Machleidt, and T. Papenbrock, *Phys. Rev. Lett.* **108**, 242501 (2012).
- [17] J.D. Holt, T. Otsuka, A. Schwenk, and T. Suzuki, *J. Phys. G* **39**, 085111 (2012).
- [18] A. T. Gallant *et al.*, *Phys. Rev. Lett.* **109**, 032506 (2012).
- [19] R. Roth, S. Binder, K. Vobig, A. Calci, J. Langhammer, and P. Navrátil, *Phys. Rev. Lett.* **109**, 052501 (2012).
- [20] B. Jurado *et al.*, *Phys. Lett. B* **649**, 43 (2007).
- [21] G. Audi, O. Bersillon, J. Blachot, and A.H. Wapstra, *Nucl. Phys. A* **729**, 3 (2003).
- [22] A. T. Reed *et al.*, *Phys. Rev. C* **60**, 024311 (1999).
- [23] M. Stanoiu *et al.*, *Phys. Rev. C* **85**, 017303 (2012).
- [24] N. Frank *et al.*, *Phys. Rev. C* **84**, 037302 (2011).
- [25] R. Anne, D. Bazin, A. C. Mueller, J. C. Jacmart, and M. Langevin, *Nucl. Instrum. Methods Phys. Res., Sect. A* **257**, 215 (1987).
- [26] J. Simpson *et al.*, *Acta Phys. Hung. New Ser.: Heavy Ion Phys.* **11**, 159 (2000).
- [27] See the Supplemental Material <http://link.aps.org/supplemental/10.1103/PhysRevLett.110.082502> for details.
- [28] M. Bellegric *et al.*, *Phys. Rev. C* **72**, 054316 (2005).
- [29] J. Gibelin *et al.*, *Phys. Rev. C* **75**, 057306 (2007).
- [30] S. W. Padgett *et al.*, *Phys. Rev. C* **72**, 064330 (2005).
- [31] W. Catford *et al.*, *Phys. Rev. Lett.* **104**, 192501 (2010).
- [32] D. R. Goosman, D. Alburger, and J. Hardy, *Phys. Rev. C* **7**, 1133 (1973).
- [33] C. Rodríguez-Tajes *et al.*, *Phys. Rev. C* **82**, 024305 (2010).
- [34] B. A. Brown and B. H. Wildenthal, *Annu. Rev. Nucl. Part. Sci.* **38**, 29 (1988).
- [35] B. A. Brown and W. A. Richter, *Phys. Rev. C* **74**, 034315 (2006).
- [36] F. Coester, *Nucl. Phys.* **7**, 421 (1958).
- [37] F. Coester and H. Kümmel, *Nucl. Phys.* **17**, 477 (1960).
- [38] S. A. Kucharski and R. J. Bartlett, *J. Chem. Phys.* **108**, 5243 (1998).
- [39] A. G. Taube and R. J. Bartlett, *J. Chem. Phys.* **128**, 044110 (2008).
- [40] G. Hagen, T. Papenbrock, D.J. Dean, and M. Jensen-Hjorth, *Phys. Rev. C* **82**, 034330 (2010).
- [41] G.R. Jansen, M. Hjorth-Jensen, G. Hagen, and T. Papenbrock, *Phys. Rev. C* **83**, 054306 (2011).
- [42] D.R. Entem and R. Machleidt, *Phys. Rev. C* **68**, 041001 (2003).
- [43] J. W. Holt, N. Kaiser, and W. Weise, *Phys. Rev. C* **79**, 054331 (2009); **81**, 024002 (2010).
- [44] Ø. Jensen, G. Hagen, M. Hjorth-Jensen, B. A. Brown, and A. Gade, *Phys. Rev. Lett.* **107**, 032501 (2011).
- [45] N. Michel, W. Nazarewicz, M. Płoszajczak, and T. Vertse, *J. Phys. G* **36**, 013101 (2009).